

# Absolute transmitted light plethysmography for assessment of dental pulp vitality through quantification of pulp chamber hematocrit by a three-layer model

Satoko Kakino

Yuzo Takagi

Tokyo Medical and Dental University  
Section of Developmental Oral Health Science  
School of Dentistry  
Tokyo, Japan

Setsuo Takatani

Tokyo Medical and Dental University  
Department of Artificial Organs  
Institute of Biomaterials and Bioengineering  
Tokyo, Japan  
E-mail: takatani.ao@tmd.ac.jp

**Abstract.** After confirming that the gingival circulation had little effect on transmitted light plethysmography measurement in the upper central incisor in both *in vivo* experiments and numerical Monte Carlo simulation studies, a three-layer model comprising of a pulp chamber sandwiched between two dentin layers has been introduced to quantify the pulp chamber hematocrit ( $Hct_p$ ) from the measured optical density. Two-flux theory was utilized to derive a mathematical equation for transmitted intensity in terms of tooth dimensions,  $Hct_p$ , and light-source wavelength. Each layer was assumed homogeneous so as to represent its optical properties by the bulk absorption and scattering constants. The mean error between the  $Hct_p$  estimate based on the three-layer-model equation and the  $Hct_p$  actual in the extracted model tooth was  $-0.00115$  with standard deviation (SD) of  $0.00733$  at  $522$  nm wavelength, while for  $810$  nm  $+0.09157$  and  $0.02493$ . The  $Hct_p$  estimate of the upper central incisor in 10 young volunteers at  $522$  nm using the three-layer model ranged from  $0.002$  to  $0.061$  with the mean of  $0.032$ . The  $Hct_p$  change reflects blood volume shift in the pulp microcirculation to possibly indicate dental pulp vitality.  
© 2008 Society of Photo-Optical Instrumentation Engineers. [DOI: 10.1117/1.2976112]

Keywords: transmitted light plethysmography; two-flux theory; dental pulp hematocrit; dental pulp microcirculation; dental pulp vitality.

Paper 07304RR received Aug. 3, 2007; revised manuscript received Apr. 29, 2008; accepted for publication May 13, 2008; published online Sep. 11, 2008.

## 1 Introduction

The vitality or wellness of the dental pulp is determined by the electric pulp testing (EPT) or thermal sensitivity test, where the sensitivity of the pulp sensory nerves to an electrical or thermal stimulus is given a score according to the patient's responses. These methods, however, may not reveal real vitality or wellness of the pulp tissue because of the indirectness and subjectivity of the modality. In addition, because the EPT relies on the patient's responses and might induce as unpleasant sensation, it could result in a false-positive outcome, particularly in young patients. In some cases, such as traumatized or young permanent teeth, false-negative outcomes have also been reported due to elevated threshold levels in the pulp nerves.<sup>1,2</sup>

Following the earlier works by Uptegrove et al.<sup>3</sup> and Beer et al.,<sup>4</sup> during 1980 to 1990s Laser Doppler flowmetry,<sup>5,6</sup> pulse oximetry,<sup>7-9</sup> and transmitted light plethysmography<sup>10,11</sup> (TLP) were investigated to noninvasively assess "pulp vitality." Among them, the TLP was found to be promising to provide information related to circulatory changes occurring inside the pulp chamber by measuring the transmitted light through a whole tooth. Toward quantitative assessment of

pulp vitality, Diaz-Arnold et al.,<sup>12,13</sup> utilizing the extracted model tooth whose pulp chamber had been filled with the bovine blood, reported that the hemoglobin content and oxygen saturation of the blood in the pulp chamber could be quantified by measuring the optical transmission at the 576, 660, and 830 nm wavelengths. It was speculated that the TLP could be used to assess pulp vitality reflected in the blood volume changes occurring in the pulp chamber synchronized with the heart beat. Contrary to the report of Diaz-Arnold et al., Fein et al. emphasized that in the middle-aged and older patients the TLP pulsation was caused by the blood volume changes in the gingiva not in the pulp chamber.<sup>14</sup> It was reported that the optical signal transmitted through the gingiva and then the tooth appeared to have topped over the signal changes occurring in the pulp chamber. The controversy of the TLP signal cause was previously addressed by our group, where the effects of the periodontal blood flow on the TLP signal amplitude were investigated by blocking the background light propagation through the periodontal tissue with an opaque rubber material placed over the gingiva.<sup>15</sup> The results, however, were not conclusive because of the constrictive force of the rubber material altering the blood flow through the gingiva. Thereafter, a series of studies had been designed (i) to verify optical propagation paths through a tooth, (ii) to develop a model in quantifying the pulp hemat-

Address all correspondence to Setsuo Takatani, Artificial Organs, Tokyo Medical and Dental University, 2-3-10 Surugadai, Kanda, Chiyoda-ku, Tokyo 101-0062, Japan; Tel: +81-3-5280-8168; Fax: +81-3-5280-8168; E-mail: takatani.ao@tmd.ac.jp

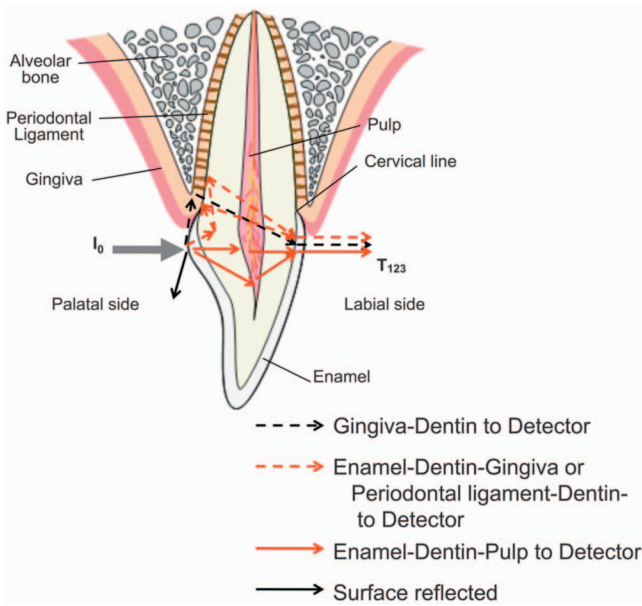


**Fig. 1** Vertically cut cross section of the upper central incisor showing its anatomical structure and possible optical paths.

ocrit in human upper central incisors based on the TLP measurement, and (iii) to validate the applicability of the TLP for assessing pulp vitality. To attain the goal, a multiwavelength TLP system was constructed to obtain a tooth's optical transmission spectrum in the visible and near-infrared regions sampled at 467, 506, 522, and 810 nm wavelengths using light-emitting diodes (LEDs).<sup>16</sup> It was demonstrated in the extracted model tooth as well as in the human volunteer studies that the pulsed LED signals of 560 Hz minimized the background light noise to enhance the signal-to-noise ratio and to obtain cleaner TLP signal.

In this study, preliminary studies, both experimental and theoretical, were conducted first to verify optical propagation paths in an upper central incisor. First, the effects of the light signal traveling on the palatal surface of the tooth, entering the gingiva, and then propagating through the tooth toward the detector placed on the labial surface were examined experimentally by blocking the transmission between the light source and gingiva with a silicone material injected around the gingival sulcus. Second, the amount of the light that had reflected off the gingiva, and periodontal ligaments inside the tooth and that had propagated toward the detector was estimated numerically by the Monte Carlo simulation.<sup>17</sup> After confirming that the gingival circulation had little affect on TLP measurement, a three-layer model comprising of a pulp chamber sandwiched between two dentin layers was then developed to quantify the transmitted light intensity in terms of (i) pulp chamber hematocrit  $Hct_p$ , (ii) tooth dimensions, and (iii) light-source wavelength. By assuming a diffuse radiation incident upon the tooth and by employing the two-flux model proposed by Kubelka,<sup>18,19</sup> a mathematical equation was developed. The accuracy of the model for estimating the  $Hct_p$  was then examined in the extracted model tooth by varying the pulp chamber size,  $Hct_p$ , and light-source wavelength. Finally, the model was applied to quantify the hematocrit of the blood in the upper central incisors of the human volunteers from



**Fig. 2** Multiwavelength optical plethysmograph.

which the volume fraction of the pulp vascular system was estimated to evaluate pulp vitality.

## 2 Studies to Verify Optical Paths in a Tooth

Referring to the anatomical structure of the upper central incisor and possible light propagation paths depicted in Fig. 1, the preliminary studies composed of (i) measurements in human volunteers to verify the effects of the light wave external to the tooth propagating to the gingiva on the TLP signal change (black broken lines in Fig. 1) and (ii) Monte Carlo simulation to quantify the effects of the light that had scattered off the gingiva and periodontal ligaments inside the tooth on the TLP signal change (red solid lines in Fig. 1).

### 2.1 Effects of Light Wave External to the Tooth Propagating Directly to Gingiva on TLP Signal

The effects of the light wave external to the tooth traveling through the gingiva on the TLP signal were examined in the human volunteers. After the protocol for human study was approved by the Institutional Review Board of the Tokyo Medical and Dental University, the optical measurements in the upper central incisor of human volunteers were conducted using the multiwavelength TLP system (Fig. 2).<sup>16</sup> Preceding the study, a resin adaptor (as shown in Fig. 3) for each subject was fabricated to fix the optical fibers against a tooth. As a light source, we used the 522 nm wavelength LED pulsed at 560 Hz. The transmitted light through the tooth at 560 Hz

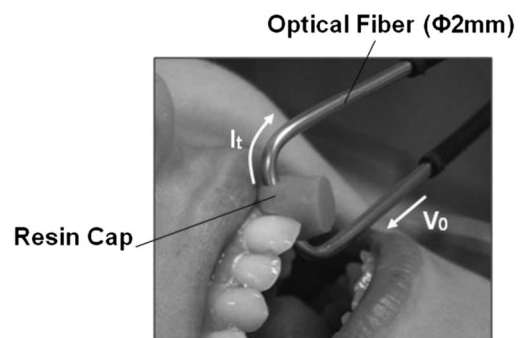


**Fig. 3** Resin cap placed on the upper central incisor with optical fibers.

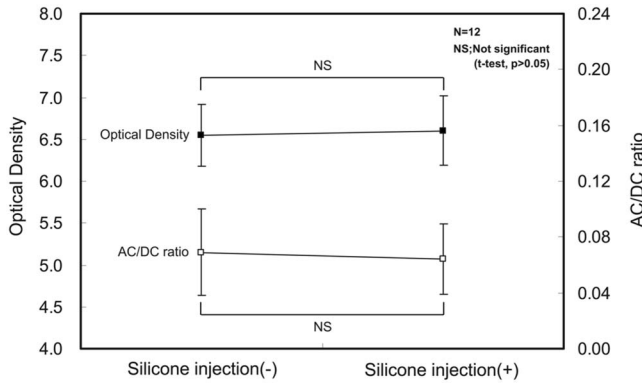


Fig. 4 OD and ac/dc ratio obtained in human volunteers showing the effects of the silicone material injected around the gingival sulcus.

was sampled to minimize the background light. At first, the dc component (absolute level of the transmitted light signal) and the ac component (periodically varying signal amplitude synchronized to heart beat) of the TLP signals at 522 nm wavelength were recorded in each subject for ~2 min. Then, the silicone impression material, Exafine Regular Type (GC Dental Products Corp., Tokyo Japan) was injected into the gingival sulcus around the resin cap and proximal surface of the tooth to block the light propagation between the optical fiber and the gingiva, followed by the recording of the dc and ac signals again. The significance in the difference between the two measurements with and without the silicone material was evaluated with  $p < 0.01$ .

Figure 4 showed the changes in dc and ac/dc signals of the TLP in the upper central incisors before and after injection of the silicone impression material ( $n=12$ , 25–31 years old with mean 27.3 years old). With the silicone injected in the gingival sulcus, the average value of the optical density (OD) changed from  $6.55 \pm 0.07$  to  $6.60 \pm 0.07$ , and ac/dc ratio changed from  $0.069 \pm 0.031$  to  $0.064 \pm 0.025$ . For both OD and ac/dc values, there were no significant differences with and without silicone impression material. This study demonstrated that the light wave traveling on the tooth surface directly from the light source to the gingiva had little affect on TLP measurements.

2.2 Monte Carlo Simulation of Light Propagation Inside the Tooth

Figure 5 showed a two dimensional Monte Carlo simulation model of the tooth Fig. 1 showing layers of enamel, dentin, pulp, and gingiva. The dimensions of the model reflect those of the average size tooth as measured using the X-ray machine (refer to Table 1 data). In the microscopic domain of dentin, each dentin layer consisted of a collagen fiber and mineral substance having a 30- $\mu\text{m}$  thickness, each with the differential optical properties between them affecting the light propagation. Table 2 shows the optical properties of the dentin material for the wavelengths of 522 and 810 nm.<sup>20</sup> The Monte Carlo simulation of the light propagation for the model tooth of Fig. 5 was derived by an iterative calculation using Eqs. (1)–(4).<sup>17</sup> The photon step size and its angle of scattering at one scattering were determined by Eqs. (1)–(3), yielding the maximum step size of photon in the mineral substance to be

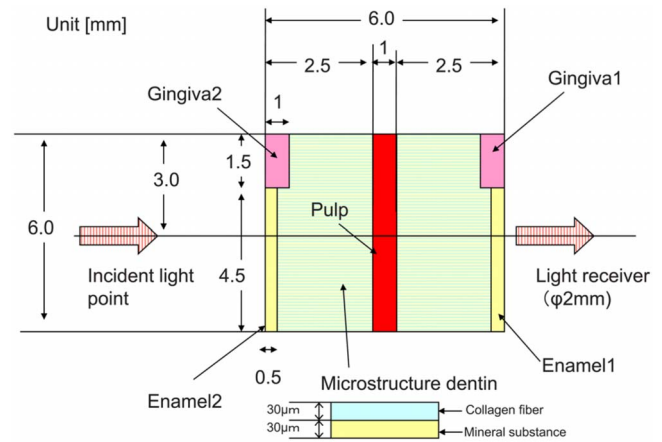


Fig. 5 Two-dimensional tooth model vertically cut in the plane of the optical fibers for the Monte Carlo simulation.

~37  $\mu\text{m}$  for 522 and 810 nm. We thus employed the mesh size of 30  $\mu\text{m}$  in the Monte Carlo simulation. The iterative equations used for calculation were

$$s = \frac{-\ln(RN_1)}{\mu_t} \tag{1}$$

$$\theta = \cos^{-1} \frac{1}{2g} \left[ \left\{ 1 + g^2 - \left( \frac{1 - g^2}{1 + g - 2gRN_2} \right)^2 \right\} \right] \tag{2}$$

$$\phi = 2\pi RN_3 \tag{3}$$

$$\mu_t = \mu_a + \mu_s, \tag{4}$$

where  $s$  is the mean free path between the scattering;  $RN_{1,2,3}$  is the random number evenly distributed between 0 and 1 and  $\mu_t, \mu_a$ , and  $\mu_s$  are the extinction, absorption, and scattering coefficient, respectively.  $\theta$ , the probability distribution for an arc-cosine of a deflection, obeys the scattering function of Henyey and Greenstein phase function.  $g$  is the anisotropy of scattering that has the value between -1.0 and 1.0, where

Table 1 Dimensions of the selected teeth.

Tooth No.	Tooth BL thickness (mm)	Pulp BL thickness (mm)
1	6.1	0.44
2	6.1	0.67
3	6.6	0.34
4-1	6.0	0.28
4-2	6.0	0.40
4-3	6.0	0.51
5	6.6	0.78

**Table 2** Optical properties of dentin and gingiva.

Light wavelength (nm)	Optical properties (mm <sup>-1</sup> )	Dentin			Gingiva
		Oxygenated blood (100%)	Mineral substance	Fiber (Spinal fluid)	
522	$\mu_s$	0.95	28.09	0.01	0.10
	$\mu_a$	42.60	0.44	0.002	4.26
	$g$	0.85	0.80	0	0.90
810	$\mu_s$	0.95	26.97	0.01	0.10
	$\mu_a$	1.46	0.34	0.002	0.15
	$g$	0.85	0.80	0	0.90

the value of 0 indicates isotropic scattering and the value near 1.0 indicates highly forward scattering.  $\phi$  is the azimuthal angle.

In order to emphasize the photon paths in the model, the result was shown by the level of absorption intensity. The numbers of photons that had scattered off the gingiva and then traveled through the tooth and those that did not reach gingiva were tracked separately to show the effects of gingiva on the transmitted light intensity. Figure 6 showed the absorbed light intensity for 522 and 810 nm wavelengths in the macroscopic scale. In Fig. 7 absorption intensities in the  $500 \times 500 \mu\text{m}$  microscopic scale were shown, where the photons scattered in the enamel layer became guided along the dentin tubule toward pulp chamber, the effect similar to that reported by Kiele and Hibst<sup>21</sup> Table 3 summarizes the statistical results showing how many photons have traveled to hit the gingiva and scattered off toward the detector. Out of 20 million photons injected inside the model tooth, only 5 photons (0.000025%) traveled to the gingiva, while 497 photons (0.0025%) at 522 nm and 876 photons (0.0044%) at 810 nm, over 100 times those that hit the gingiva, traveled through pulp to the detector without routing the gingiva. The Monte Carlo simulation has thus indicated the minimal effects of the gingival circulation on the optical transmission measurements in an upper central incisor model.

### 3 Theoretical Model for the Human Upper Central Incisors

Because the results in the preliminary studies showed that the transmitted light intensity through an upper central incisor was little affected by the gingival circulation, we proceeded with the development of a theoretical model to quantify pulp hematocrit so as to evaluate pulp vitality.

#### 3.1 Dentin-Pulp Chamber-Dentin Three-Layer Model

The tooth structure was simplified to a three-layer model comprising of dentin-pulp chamber-dentin layers (Fig. 8). Although there are paths around the pulp chamber for the photons to propagate, the tubules in the dentin layer are organized in such a way to guide the light toward the pulp chamber.<sup>21</sup> The Monte Carlo simulation presented above supported the

light-guiding phenomenon, as illustrated in the microscopic absorption intensity in the dentin model. The scattering property of the dentin layer is so much greater than that of the enamel layer that the tooth appearance is determined mainly by the scattering property of the dentin tubules.<sup>22,23</sup> The exclusion of the enamel layer from the model thus does not affect the relative changes of the model performances in terms of the red blood cell concentration inside the pulp chamber.

#### 3.2 Three-Layer Model (TLM) Equation

In deriving a mathematical equation for the transmitted light intensity through a three-layer model (TLM), we assumed that each layer was homogeneous and also the diffuse radiation was incident upon the medium so as to justify the application of the two-flux model introduced by Kubelka with no reflection at the layer boundary (Fig. 9).<sup>18</sup> The differential equations for the two fluxes,  $I$  in the positive direction and  $J$  in the negative direction are written as

$$\frac{dI}{dx} = -(S + K)I + SJ \quad (5)$$

$$\frac{dJ}{dx} = (S + K)J - SI \quad (6)$$

with boundary conditions at  $x=0$  and  $x=d$

**Table 3** Results of the Monte Carlo simulation.

Wavelength	Number of transmitted photons (Incident photon number=20,000,000)	
	Scattered by the gingiva	No scattering at gingiva
522 [nm]	5(0.000025%)	497(0.0025%)
810 [nm]	17(0.000085%)	876(0.0044%)

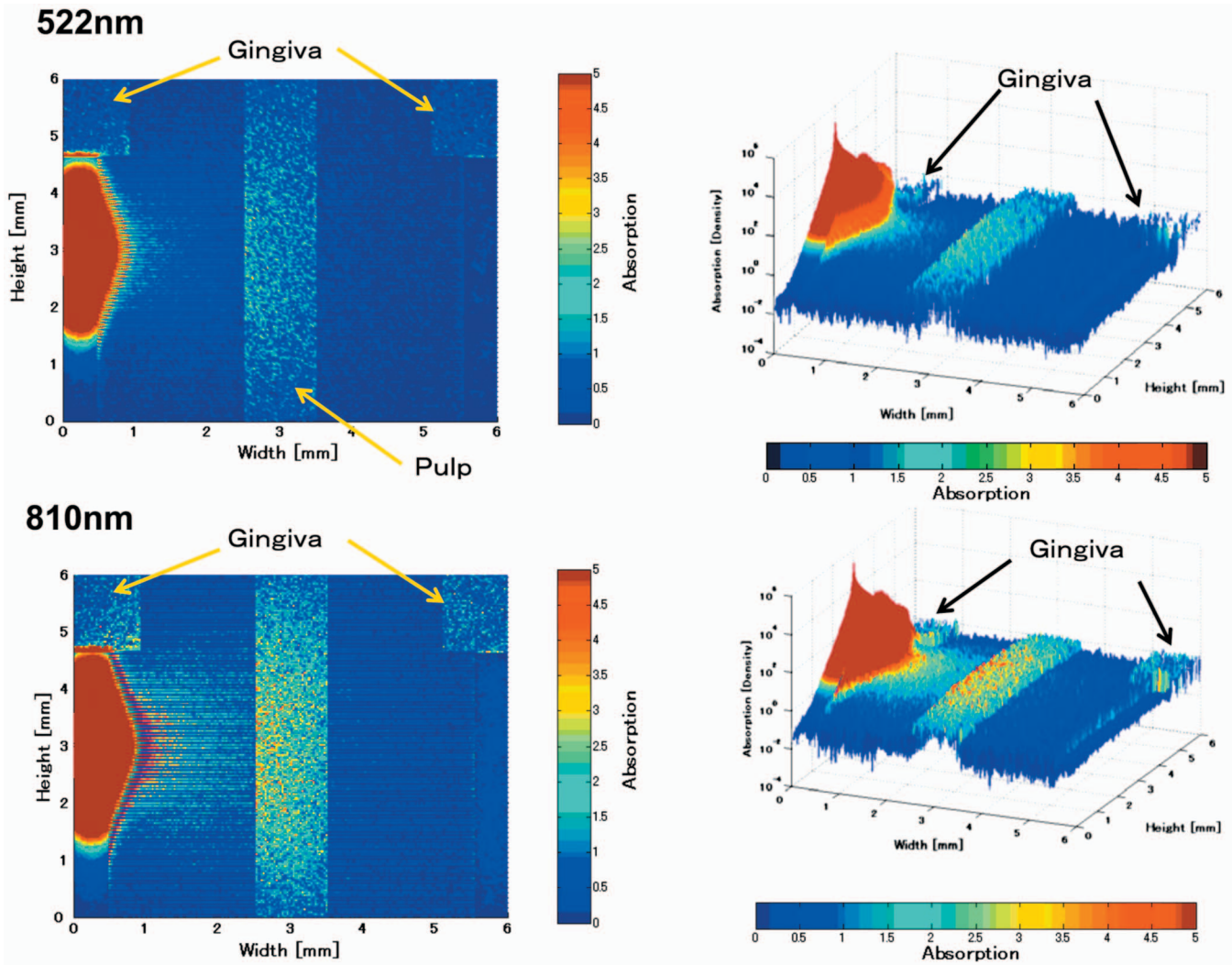


Fig. 6 Absorption intensity for 522 nm and 810 nm obtained by the Monte Carlo simulation. Left side are two-dimensional plots and right side three-dimensional plots.

$$J(x = d) = 0$$

$$I(x = 0) = I_0.$$

In Eqs. (5) and (6),  $S$  and  $K$  are the scattering and absorption constants of the medium in  $\text{mm}^{-1}$ . The solutions for Eqs. (5) and (6) in the form of the transmittance and reflectance,  $T$  and  $R$ , are given as<sup>18</sup>

$$T = \frac{b}{a \sinh(bP) + b \cosh(bP)} \quad (7)$$

$$R = \frac{1}{a + b \operatorname{ctgh}(bP)}, \quad (8)$$

where

$$a = \frac{S + K}{S}, \quad b = (a^2 - 1)^{1/2} \quad (9)$$

$$P = Sd, \quad d: \text{thickness of the layer.} \quad (10)$$

Now we consider when three homogeneous layers with different optical properties were next to each other as shown in Fig. 10. The solution can be given in a closed form as a function of the transmittance and reflectance of each layer as follows:<sup>19</sup>

$$T_{123} = \frac{T_1 T_2 T_3}{1 - R_1 R_2 - R_2 R_3 + R_1 R_2^2 R_3 - R_2 T_2 R_3}, \quad (11)$$

where  $T_{123}$  is the transmittance through the layers 1, 2, and 3,  $T_1, T_2, T_3$  the transmittance and  $R_1, R_2, R_3$  the reflectance of the layer 1, 2, and 3, respectively, computed using Eqs. (7)–(10) with appropriate  $S$  and  $K$  values and the thickness of each layer.

### 3.3 Optical Constants of Dentin and Pulp Chamber

The scattering and absorption properties of the medium are wavelength dependent, particularly of hemoglobin contained

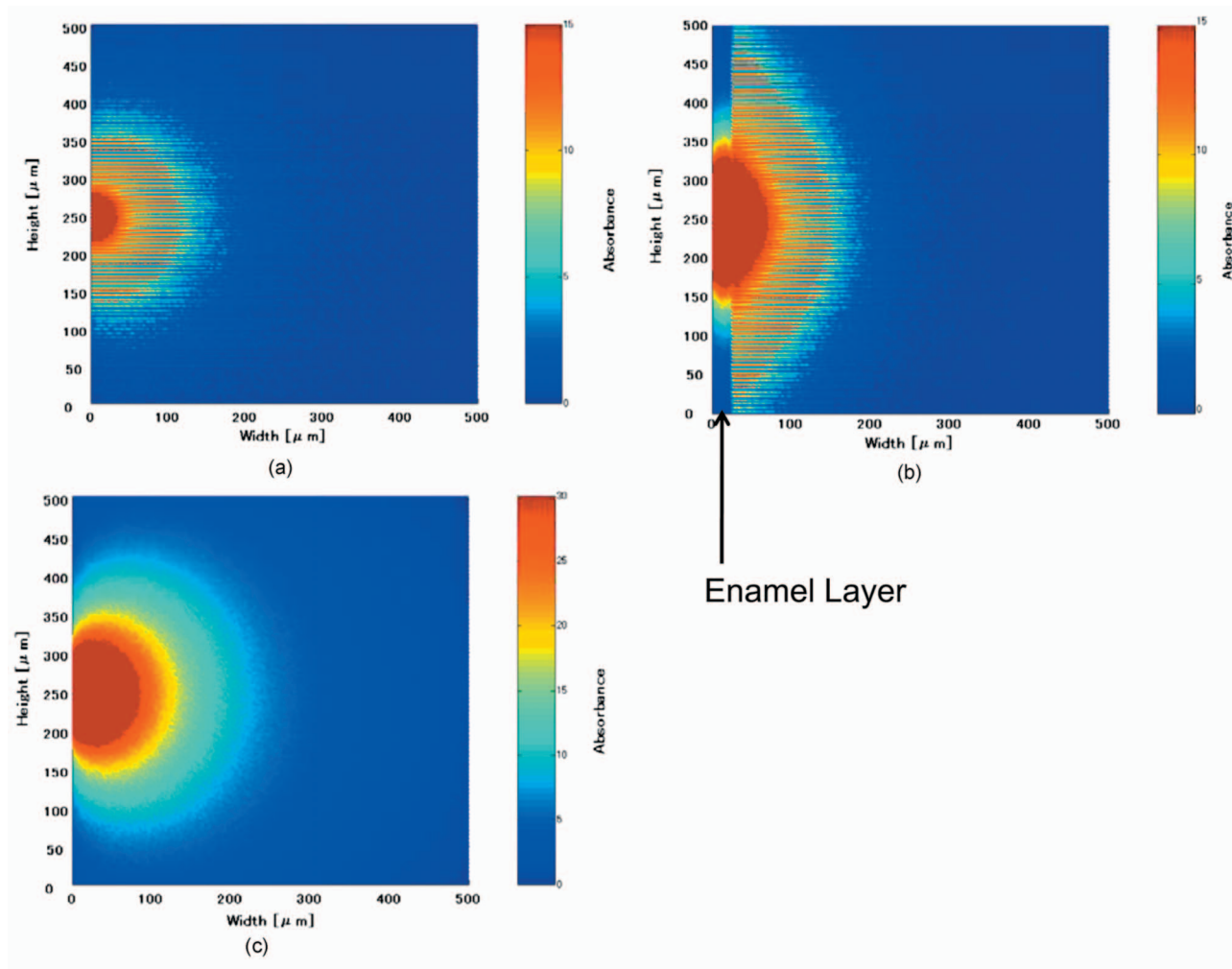


**Fig. 7** Microscopic absorption intensity for 522 nm (top) and 810 nm (bottom) in the left panel without enamel layer. In the right panel, for 522 nm, with the enamel layer, the scattered light in the enamel layer was directed along the dentin tubules with the highest intensity at the center.

inside the red blood cells. In this study, the transmission through three layers  $T_{123}$  was computed for the isosbestic wavelengths of the oxy- and deoxy-hemoglobin, in the green region at 522 nm and the near-infrared region at 810 nm [Fig. (11)].<sup>24</sup>

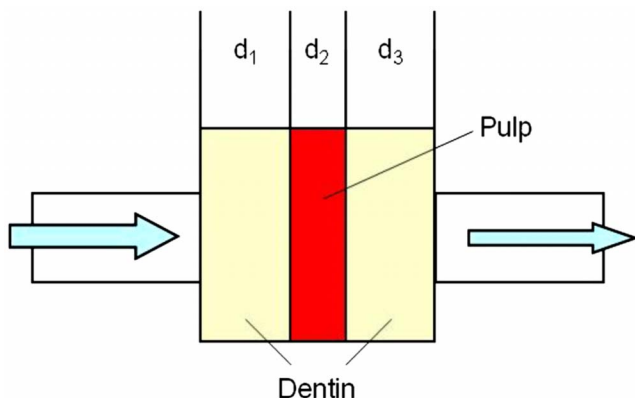


**Fig. 8** Simplified TLM consisting of dentin, pulp, and dentin layers.

For the absorption and scattering constants of the dentin layer,  $K_d$  and  $S_d$ , though its properties are dependent on the density of tubules, in this study we adopted  $K_d=0.40 \text{ mm}^{-1}$ ,  $S_d=28.09 \text{ mm}^{-1}$  for 522 nm, and  $K_d=0.344 \text{ mm}^{-1}$ ,  $S_d=26.97 \text{ mm}^{-1}$  for 810 nm, as reported by Fried et al.<sup>25</sup>

As for the optical constants of the pulp chamber, we assumed that the chamber was a homogeneous medium comprising of the whole blood. The scattering and absorption constants of the pulp chamber,  $S_b$ ,  $K_b$ , were thus derived from the optical constants of the whole blood. According to Twersky,<sup>26</sup>  $S_b$  can be derived from the scattering and absorption cross sections of a red blood cell,  $\sigma_s$  and the red blood cell concentration given by  $\text{Hct}_p/V_{\text{rbc}}$ , where  $\text{Hct}_p$  and  $V_{\text{rbc}}$  the hematocrit of the blood in the pulp chamber and the mean corpuscular volume of red blood cells, respectively, as follows:

$$S_b = \sigma_s \frac{\text{Hct}_p}{V_{\text{rbc}}} (1.0 - \text{Hct}_p). \quad (12)$$

Because the scattering in the whole blood occurs at the plasma and red blood cell interface and the scattering does not take place when  $\text{Hct}_p=0.0$  or  $1.0$ , Eq. (12) contains the factor

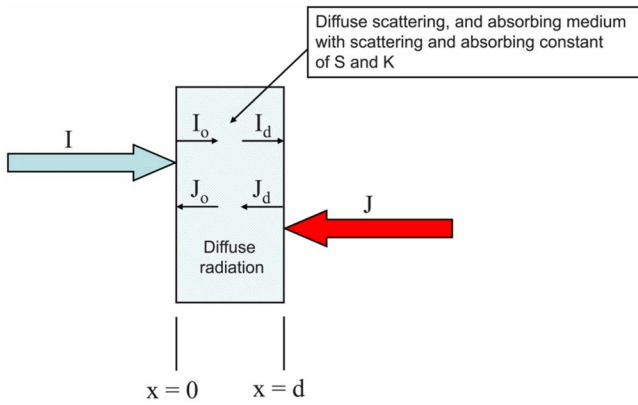


Fig. 9 Two flux model for diffuse radiation incident on a homogeneous medium.

$Hct_p (1.0 - Hct_p)$  to express nonlinear dependency of scattering on the  $Hct_p$ . Although Eq. (12) indicates that the maximum value of  $S_b$  occurs when  $Hct_p = 0.50$ , usually the  $S_b$  maxima is shifted toward lower  $Hct_p$  value at  $\sim 0.10$ .<sup>27</sup> Thus, in the calculation, the fifth-order regression equation was used to obtain a more practical value of  $S_b$  in the pulp chamber, denoted as  $S_p$ ,

$$S_p = \frac{\sigma_s}{V_{rbc}} (1002.7Hct_p^5 - 1501.6Hct_p^4 + 846.2Hct_p^3 - 218.0Hct_p^2 + 22.8Hct_p + 0.033). \quad (13)$$

The  $\sigma_s$  value of the red blood cell is dependent on the relative ratio of the red blood cell size  $V_{rbc}$  to the wavelength. The Mie theory, which treats a red blood cell as a sphere, gives the scattering cross sections of 56.8 and 31.4  $\mu m^2$  for the wavelength of 522 and 810 nm, respectively.<sup>28</sup>

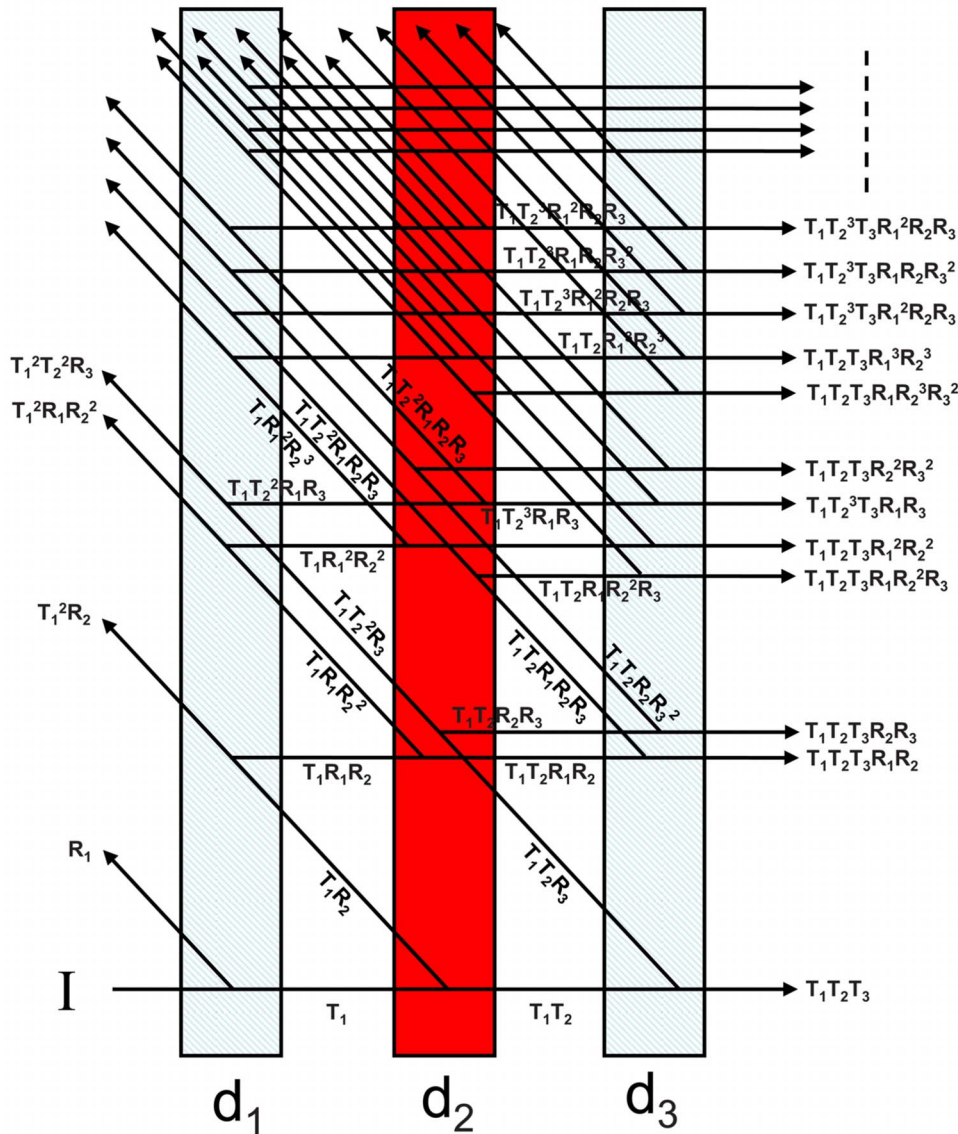


Fig. 10 TLM with the transmitted and reflected light fluxes.

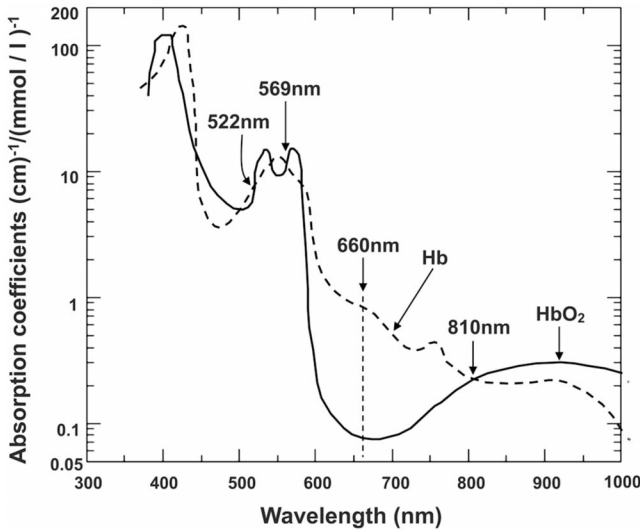


Fig. 11 Absorption coefficients of the human oxygenated and deoxygenated hemoglobin in the visible and near-infrared regions.

As for  $K_b$  value,  $\sigma_a$  is usually expressed as a linear sum of the absorption cross section of the oxygenated and deoxygenated red blood cell,  $\sigma_{ao}$ ,  $\sigma_{ar}$ , and oxygen saturation  $SO_2$  and red blood cell concentration  $Hct_p/V_{rbc}$  as follows;<sup>28</sup>

$$K_b = \frac{Hct_p}{V_{rbc}} [\sigma_{ao} SO_2 + \sigma_{ar} (1.0 - SO_2)]. \quad (14)$$

At the isosbestic wavelengths of 522 and 810 nm used in this study, the absorption does not depend on  $SO_2$  and Eq. (14) reduces to

$$K_{p,iso} = \frac{Hct_p}{V_{rbc}} \sigma_{iso}, \quad (15)$$

where  $K_{p,iso}$ ,  $\sigma_{iso}$  are the absorption coefficient of the blood in pulp chamber (in  $mm^{-1}$ ) and absorption cross section of the red blood cells (in microns squared) at the isosbestic wavelength, respectively. Figure 11 showed the absorption spectra of oxygenated and deoxygenated hemoglobin in the visible and near-infrared wavelengths.<sup>24</sup>

### 3.4 Experimental Verification of the Three-Layer Model

The experiments consisted of (i) selection of the human upper central incisors for optical measurements, (ii) transmitted optical intensity measurements in the selected sample tooth to obtain relationship between the tooth's OD versus pulp chamber hematocrit  $Hct_p$ , and to verify the accuracy of the TLM for estimation of  $Hct_p$ , (iii) microscope examination of the light propagation through a tooth to provide the basis for OD versus  $Hct_p$  relationships obtained in (ii), and (iv) optical measurements in human volunteers to quantify the hematocrit of the tooth using the TLM.

#### 3.4.1 Selection of the sample teeth

In selecting the tooth for optical measurements, the mesiodistal (MD) width and buccolingual (BL) thickness of the 25

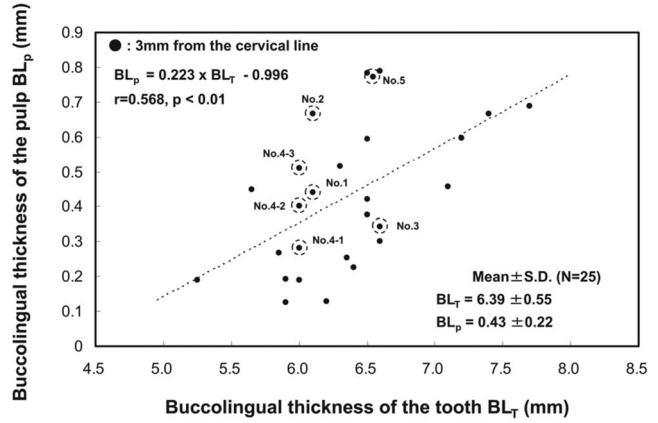


Fig. 12 Scatter plot between the BL thickness of the pulp chamber ( $BL_p$ ) versus BL thickness of the whole tooth  $BL_T$ .

extracted human upper central incisors free of caries, restoration, attrition, and discoloration were measured at 3 mm from the cervical line (Fig. 1) using X-ray equipment, Compuray (Yoshida Dental Mfg., Co. Ltd., Tokyo, Japan). Figure 12 showed the scatter plots of the BL thickness of the pulp chamber ( $BL_p$ ) vs. BL thickness of the tooth ( $BL_T$ ) with a linear regression line  $BL_p(mm) = 0.223 \times BL_T(mm) - 0.996$  ( $r = 0.568, p < 0.01$ ). Out of 25 samples, five teeth (Nos. 1–5) were selected for optical measurements. Table 1 summarized  $BL_T$  and  $BL_p$  of the selected five teeth. As for tooth 4, the pulp chamber was enlarged twice during the optical measurements denoted as Nos.4-1, 4-2, and 4-3, each having different pulp chamber size to see the effects of the pulp chamber size on the OD.

In order to introduce the blood into the pulp chamber, the root of all the sample teeth was cut off approximately 3.0 mm from the root apex. The root canal was enlarged to 1.5 mm diam, and the remnant pulp tissues were removed.

#### 3.4.2 Optical measurements in the selected teeth

A resin cap was prepared for each tooth to support the tooth as well as to fix the optical fibers as shown in Fig. 13. Two plastic optical fibers (2.0 mm diam and 1.0 m length each), one for transmitting the light signal from the LED to the tooth and the other for carrying the transmitted light signal from the tooth to a photodiode located in the multiwavelength optical plethysmograph,<sup>16</sup> were aligned perpendicular to the longitudinal axis of the tooth illuminating from the palatal surface and collecting the transmitted light from the labial surface.

The pulp chamber was filled with saline first to obtain the reference signal, followed by the measurement with the human blood having different  $Hct_p$ . After obtaining the informed consent, ~10 ml of fresh human blood was withdrawn from one of the volunteers, anticoagulated with heparin (5000 units/5 ml, Mochida Pharmaceutical Co., Ltd., Tokyo, Japan), centrifuged, and rinsed by phosphate buffer solution (PBS). The hematocrit of the blood was adjusted by adding PBS from 0.35, 0.30, 0.20, 0.10, 0.05, 0.03 to as low as 0.01. The optical measurements were made at 522 and 810 nm wavelengths. For each wavelength, the incident light intensity  $V_0$  in voltage was derived from the LED current level, while the transmitted light intensity  $V_t$  in voltage was recorded to

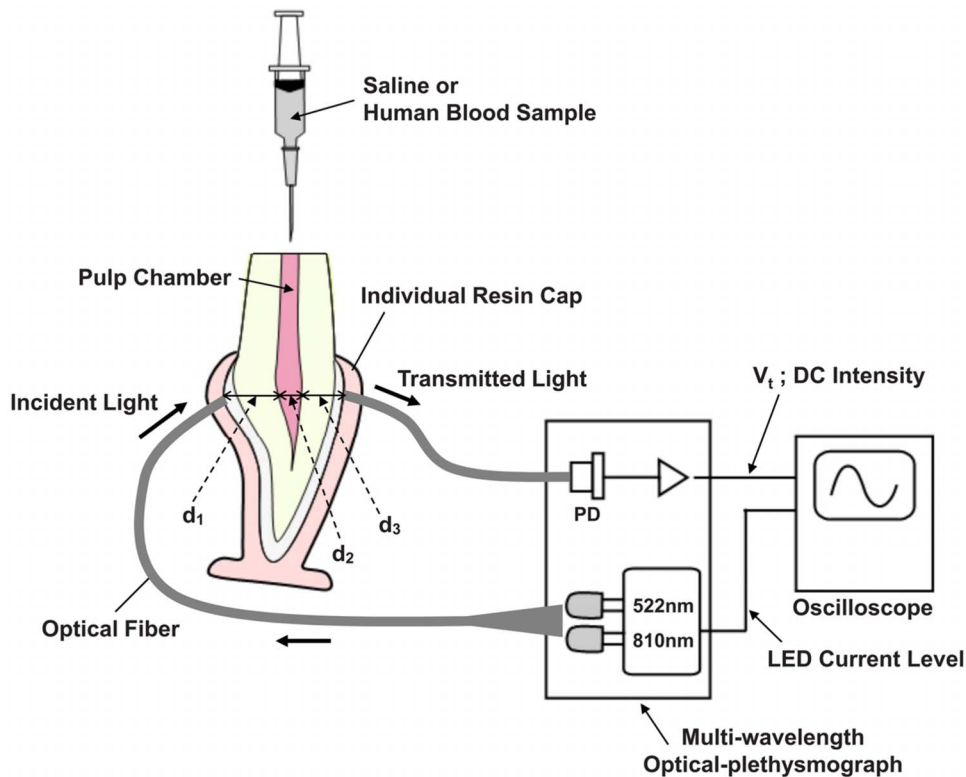


Fig. 13 Experimental setup for the optical transmission measurements in a extracted model tooth.

derive the optical density defined as  $OD = \ln(v_o/v_c)$ . The OD measurements were repeated seven times for each wavelength with different LED current levels and the data were expressed as mean  $\pm$  SD.

### 3.4.3 Examination of the optical propagation through a tooth

Following the OD measurement, the optical propagation through a tooth was examined under a microscope to verify the experimental results obtained in Sec. 3.4.2. One of the extracted human upper central incisors was cut horizontally at the plane of the incident light  $I_o$ , placed under a surgical microscope with the cut surface upward and illuminated from the palatal side with the 522 nm wavelength light using an optical fiber, as shown in Fig. 14 to observe the optical propagation process in the tooth close to the cut surface. The microscope pictures of the pulp chamber being filled with (a) saline, whole blood having hematocrit of (b) 0.03, or (c) 0.30 were obtained to elucidate the causes for the OD versus  $Hct_p$  curves. In addition, the blood was hemolyzed to reduce scattering and the hemoglobin solution equivalent to the cases of (b) or (c) were introduced into the pulp chamber to examine the effect of red blood cell scattering on the OD versus  $Hct_p$  curves obtained in Sec. 3.4.2.

### 3.4.4 $Hct_p$ estimation in the extracted model tooth

*Calibration procedure.* From the preliminary study we confirmed qualitative agreement between the TLM and the experimental results, but there was a discrepancy in the absolute levels. To utilize the TLM for quantification of the  $Hct_p$ , the

discrepancy in the absolute signal levels between the TLM and the experimental data was compensated for by using the experimental data. The OD versus  $Hct_p$  data of the reference tooth 4-2 (6.0 mm  $BL_T$  and 0.40 mm  $BL_p$ ), which was closest to the regression line of Fig. 12 was used to adjust the absolute OD level derived by the TLM. The gain constants for

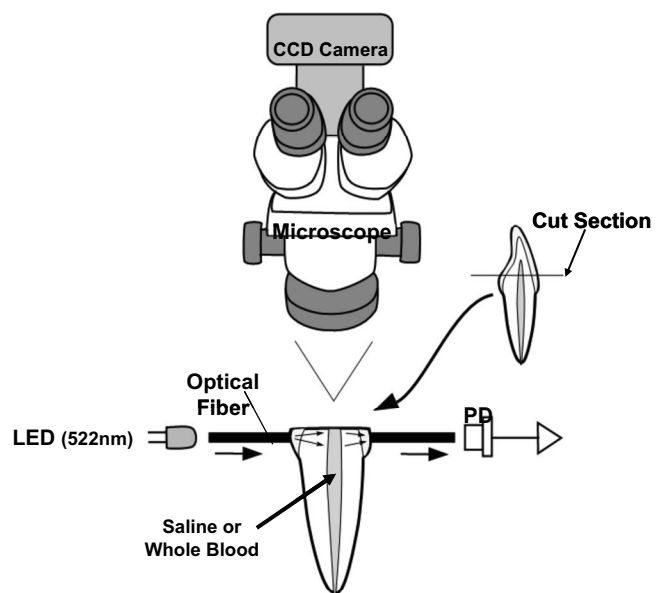
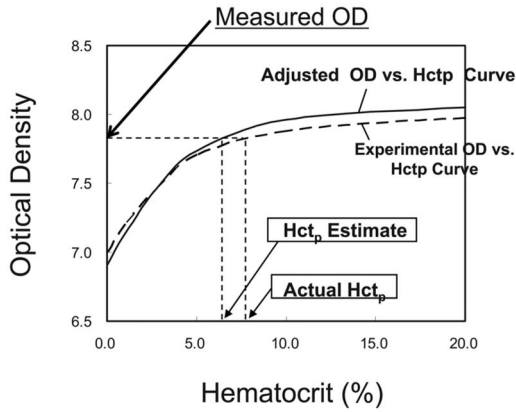


Fig. 14 Experimental setup for examining optical propagation patterns in an extracted model tooth under a microscope.



**Fig. 15** Graphical representation of how to determine  $Hct_p$  estimate from the TLM calculation and experimental OD measured in a tooth.

the saline and blood samples, denoted as  $G(0)$  and  $G(Hct_p)$ , were both defined as follows:

$$G(0) = \frac{OD_{EX-4-2}(Hct_p = 0)}{OD_{TLM-4-2}(Hct_p = 0)} \quad (16)$$

$$G(Hct_p) = \frac{OD_{EX-4-2}(Hct_p) - OD_{EX-4-2}(Hct_p = 0)}{OD_{TLM-4-2}(Hct_p) - OD_{TLM-4-2}(Hct_p = 0)}. \quad (17)$$

Here,  $OD_{EX-4-2}(Hct_p)$ ,  $OD_{EX-4-2}(Hct_p = 0)$  corresponded to the OD measurements in tooth 4-2 as a function of  $Hct_p$  and saline, respectively, while  $OD_{TLM-4-2}(Hct_p)$ ,  $OD_{TLM-4-2}(Hct_p = 0)$  the OD calculated by the TLM for reference tooth 4-2 as a function of  $Hct_p$  and saline, respectively.

*Hct<sub>p</sub> Estimation.* In obtaining  $Hct_p$  estimate from the OD data measured in the selected teeth (1, 2, 3, 4-1, 4-3, and 5), the  $OD_{TLM}(T, Hct_p)$  was first calculated for each tooth (where  $T$  is the tooth number) as a function of  $Hct_p$ , then its absolute level was adjusted using the gain constants as follows;

$$\begin{aligned} OD'_{TLM}(T, Hct_p) &= [OD_{TLM}(T, Hct_p) - OD_{TLM}(T, Hct_p \\ &= 0)]G(Hct_p) + OD_{TLM}(T, Hct_p = 0)G(0). \end{aligned} \quad (18)$$

In Eq. (18),  $OD'_{TLM}(T, Hct_p)$  is the adjusted absolute OD level by the TLM,  $G(Hct_p)$ ,  $G(0)$  the gain constants defined by Eqs. (16) and (17). The estimation of the  $Hct_p$  was carried out graphically as shown by Fig. 15 to determine the  $Hct_p$  value, where the adjusted OD curve by the TLM crossed the measured OD line. The accuracy of the method was quantified for both 522 and 810 nm wavelengths for the  $Hct_p$  values below 0.10.

### 3.4.5 Optical measurements in human volunteers

After the protocol for human study was approved by the Institutional Review Board of the Tokyo Medical and Dental University, the optical measurements in the upper central incisor in a total of 10 volunteers were conducted using the multiwavelength TLP system (Fig. 2). Prior to the study, the

purpose of the study was clearly explained and the informed consent form was signed by each volunteer. Preceding the study, a resin adaptor for each subject was fabricated to fix the optical fibers against the upper central incisor as shown in Fig. 3. The measurements were made at 522 and 810 nm. The finger-tip optical plethysmogram was also recorded to obtain the heartbeat signal. The venous blood sample of 10 ml was acquired from each volunteer to measure the systemic hematocrit.

The dimensions of each tooth, BL thickness, and MD width, were measured from the plaster model made prior to the study. As for the  $BL_p$ , we used the linear regression equation between the  $BL_T$  and  $BL_p$  obtained earlier (Fig. 12). From the measured OD values in each subject, the  $Hct_p$  was estimated using the methodology defined in Sec. 3.4.4. The gain constants  $G(0)$  and  $G(Hct_p)$  (Eqs. (16) and (17)) obtained using the reference tooth data were used first to adjust the absolute levels of the OD computed by the TLM for the  $BL_T$  and the estimated  $BL_p$  in each subject.

## 4 Results

### 4.1 Experimental Verification of the Three-Layer Model

#### 4.1.1 OD versus $Hct_p$ in the extracted model tooth

The OD changes of tooth 4 versus  $Hct_p$  were shown in Fig. 16 when the  $BL_p$  was varied from 0.28, 0.40, to 0.51 mm. The OD at 522 nm increased greatly as the  $Hct_p$  increased from 0.0 to around 7.0–8.0% with a small increase beyond that. The OD change of 810 nm, on the other hand, was much milder than that of 522 nm wavelength for the entire range of  $Hct_p$ . As for the effects of the  $BL_p$  size on the OD level, the OD increased at both 522 and 810 nm wavelengths due to increased light loss when the pulp chamber was enlarged.

Figure 17 showed the OD changes versus  $Hct_p$  for two different tooth samples, tooth 1 with smaller pulp chamber, while tooth 5 with a larger chamber from Fig. 12. Similar patterns were observed at both 522 and 810 nm wavelengths, although the OD level of saline did not agree between the two samples due to differences in the optical characteristics of the tooth material. For a smaller pulp chamber like in tooth 1, the absolute level of the OD was smaller with less light attenuation in the pulp chamber.

#### 4.1.2 Optical propagation in a tooth

Figure 18 showed the microscope pictures of the light propagation through the tooth seen from the top as the pulp chamber was filled with (a) saline, and the blood having the  $Hct_p$  of (b) 0.03 and (c) 0.30, or hemoglobin solution with hemoglobin content of (d) 1.2 g/dL or (e) 10.0 g/dL. The corresponding OD versus  $Hct_p$  curves was shown in Fig. 19 to connect the external measurement to the internal optical process.

### 4.2 Accuracy of the Three-Layer Model (TLM)

#### 4.2.1 OD versus $Hct_p$ by the TLM

In Fig. 20, OD versus  $Hct_p$  obtained by the TLM for the wavelengths of 522 and 810 nm were shown to simulate the

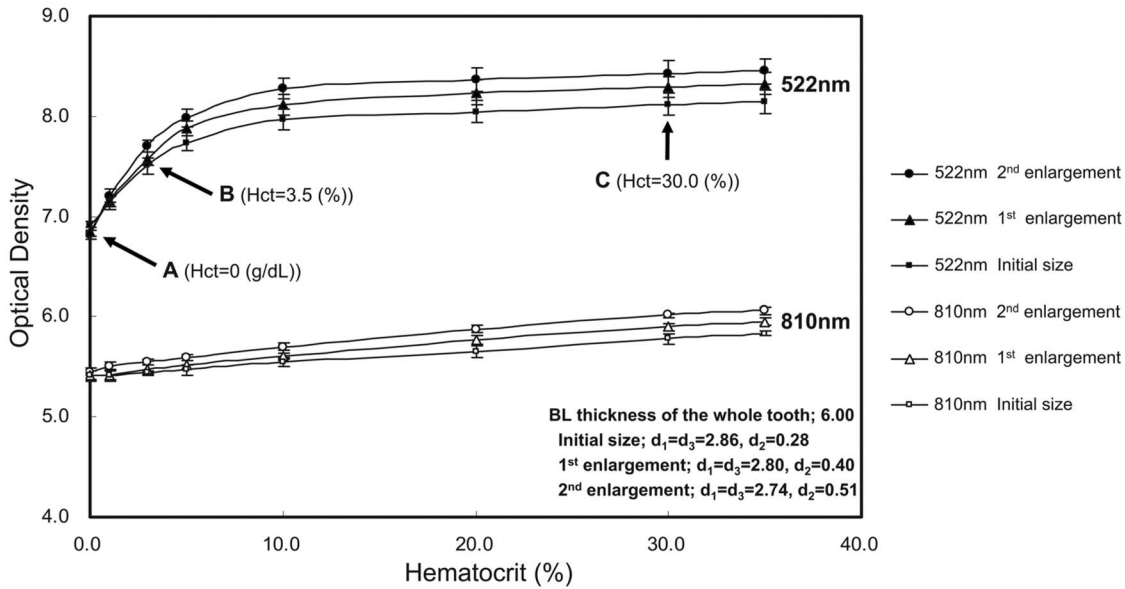


Fig. 16 OD versus  $Hct_p$  in tooth 4 for 522 and 810 nm wavelengths showing the effects of the pulp canal enlargement on the measured OD.

results of tooth 4 when the  $BL_p$  varied from 0.28, 0.40 to 0.51 mm. The TLM results agreed qualitatively with the experimental results shown in Fig. 16.

#### 4.2.2 $Hct_p$ estimation in the extracted model tooth

Figures 21(a) and 21(b) showed the scatter plot between the  $Hct_p$  estimates by the TLM versus the actual  $Hct_p$  measured in the extracted model tooth at 522 nm [Fig. 21(a)] and at 810 nm [Fig. 21(b)]. Although the error bars increased with the increase in  $Hct_p$ , the mean of the  $Hct_p$  estimate versus actual  $Hct_p$  showed an excellent agreement with the correlation coefficient of 0.957 ( $p < 0.0001$ ) for 522 nm, while

$r = 0.849$  ( $p < 0.0001$ ) for 810 nm wavelength. Figures 22(a) and 22(b) showed the mean and SD of the errors between the  $Hct_p$  estimate and the actual  $Hct_p$  for 522 [Fig. 22(a)] and 810 nm [Fig. 22(b)] wavelengths. The mean error for 522 nm was  $-0.00115$  with SD of 0.00733, while for 810 nm they were  $+0.09157$  and 0.02493.

#### 4.2.3 $Hct_p$ estimation in human volunteers

Table 4 is the summary of the *in vivo* measurements in a total of 10 volunteers with the mean age of 27.4 (from 25 to 35 years old). There were seven males and three females. The mean  $BL_T$  was 5.5 mm with the mean  $BL_p$  being 0.26 mm.

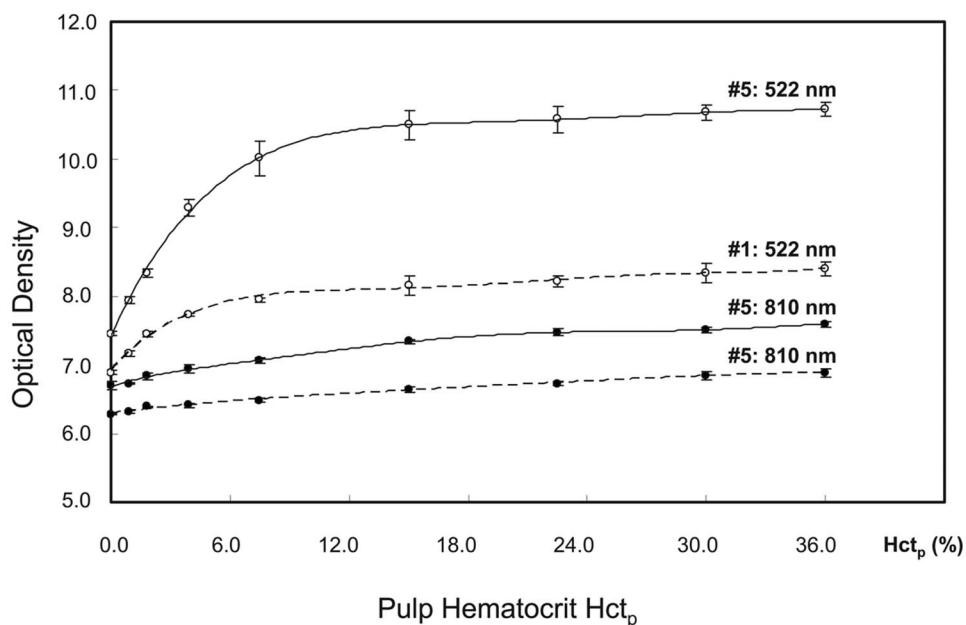
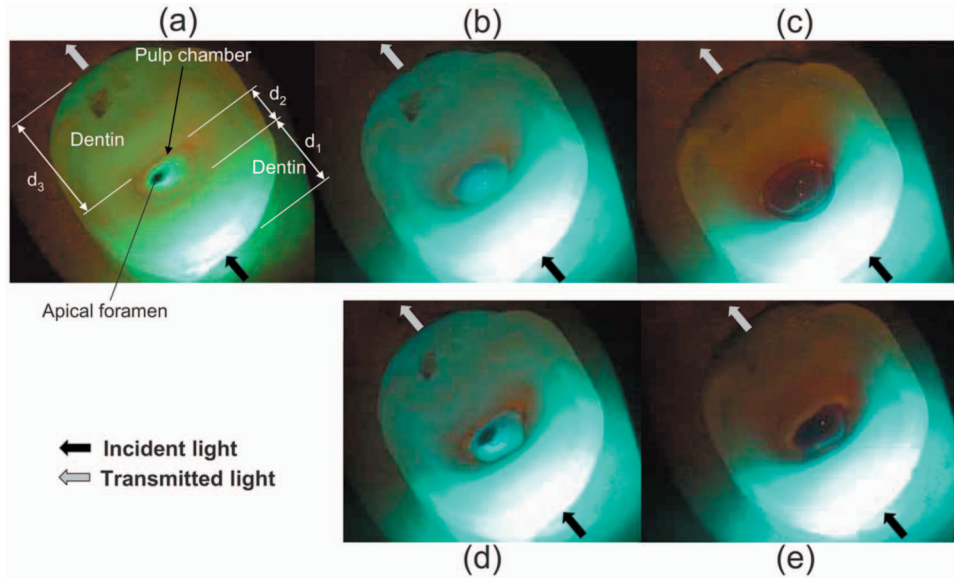


Fig. 17 OD versus  $Hct_p$  of two different extracted teeth showing the discrepancy in the OD level with saline in the pulp chamber.



**Fig. 18** Microscope pictures showing (a) optical propagation patterns with saline in the pulp chamber, (b) with 3.0% Hct<sub>p</sub> blood in the pulp chamber, and (c) with 30.0% blood in the pulp chamber. (d) and (e) show the propagation patterns when the blood of (b) and (c) was hemolyzed to reduce scattering effects.

The OD of 522 nm ranged from 6.163 to 7.889 with the mean of 7.054. The Hct<sub>p</sub> estimate using the TLM ranged from 0.002 to as high as 0.061 with the mean of 0.032. The estimation of Hct<sub>p</sub> using 810 nm was not quite successful as 522 nm, except in a few subjects.

## 5 Discussion

Our preliminary experimental and theoretical studies both revealed that the transmitted-light signal changes detected from the labial side of the upper central incisor were not affected by

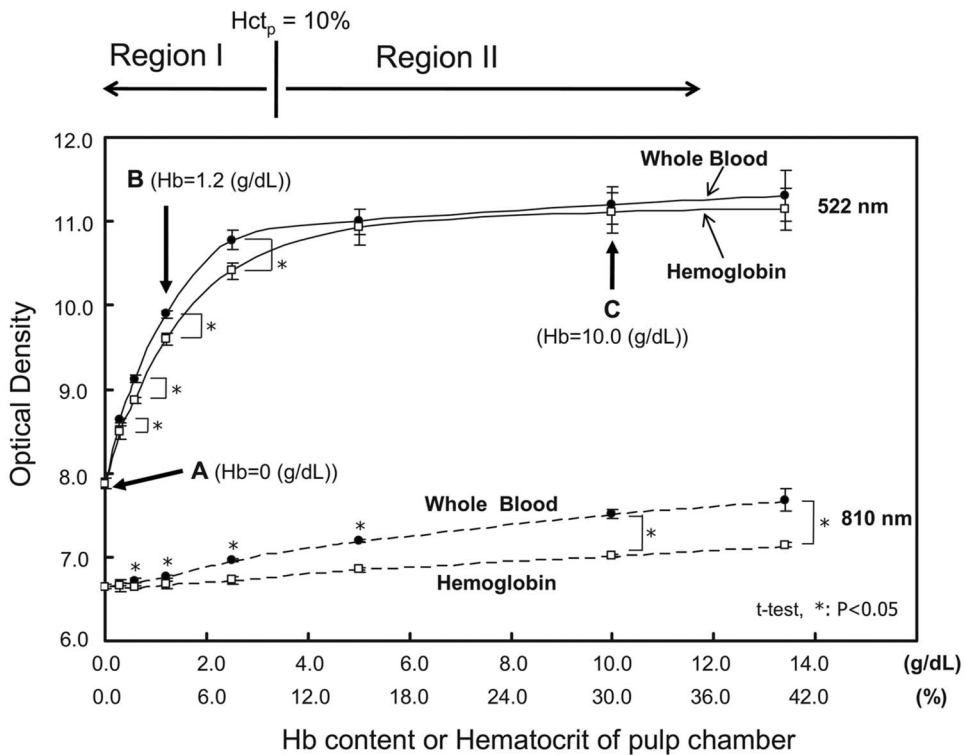


**Fig. 19** OD versus Hct<sub>p</sub> or hemoglobin content showing the effects of scattering in the extracted model tooth when the pulp chamber was filled with whole blood or hemoglobin solution.

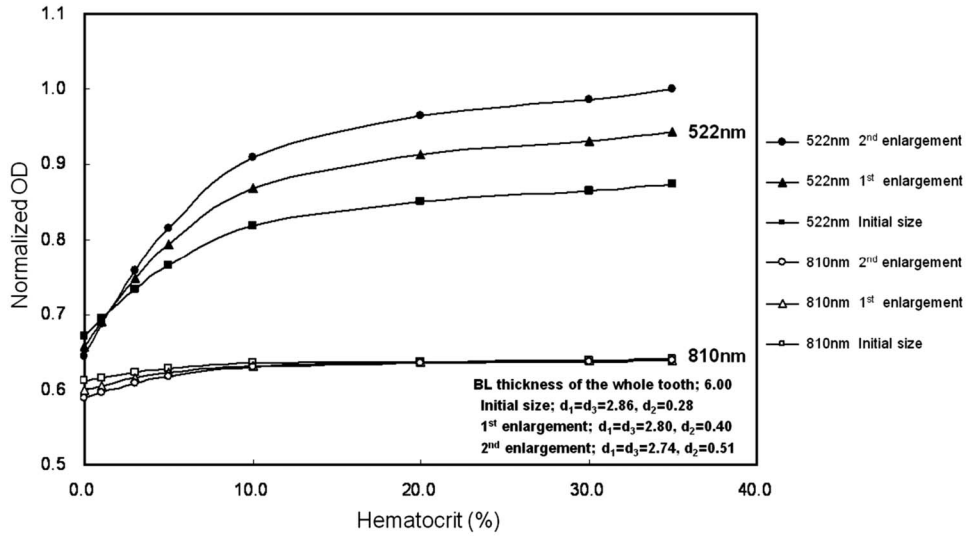
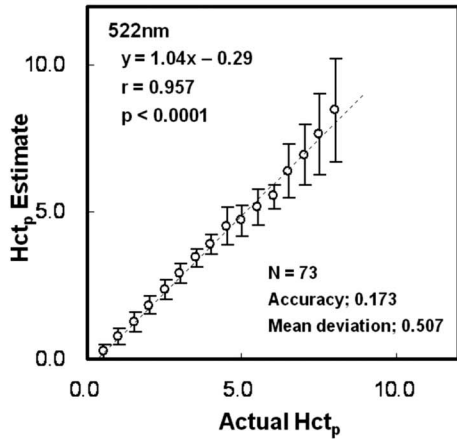
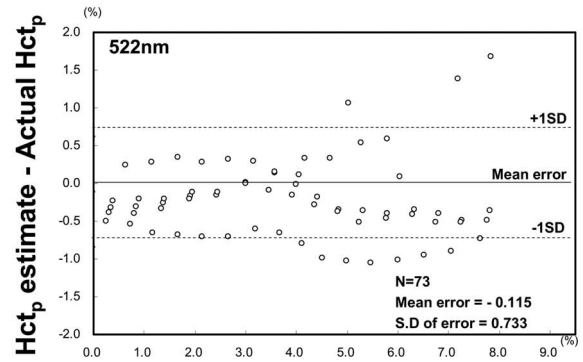


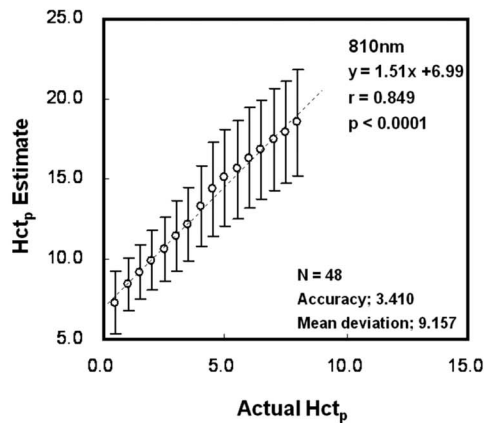
Fig. 20 OD versus Hct<sub>p</sub> of the tooth 4 for varying pulp chamber size generated by the TLM.



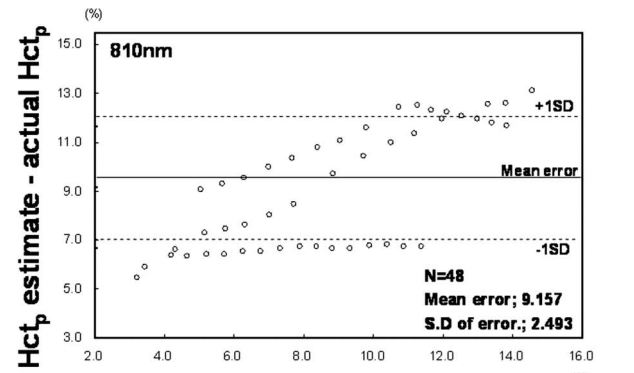
(a)



(a)



(b)



(b)

Fig. 21 Scatter plots between the Hct<sub>p</sub> estimate by the TLM and the Hct<sub>p</sub> actual in the extracted model tooth for (a) 522 nm and (b) 810 nm.

Fig. 22 Bland and Altman plots showing distribution of errors between the Hct<sub>p</sub> estimate and the Hct<sub>p</sub> actual in the extracted model teeth for (a) 522 nm and (b) 810 nm light-source wavelength.

**Table 4** Summary of the *in vivo* optical measurements.

Subject	Age	M/F	R/L	BL <sub>T</sub> (nm)	BL <sub>P</sub> (nm)	H <sub>sys</sub>	OD		Hct <sub>p</sub> Estimate		BV <sub>F</sub>	
							522 nm	810 nm	522 nm	810 nm	522 nm	810 nm
A	25	M	R	5.7	0.28	0.47	7.377	5.945	0.042	—	0.177	—
			L	6.1	0.36	0.47	7.405	5.974	0.002	—	0.010	—
B	25	M	R	5.7	0.28	0.48	7.345	5.866	0.040	—	0.168	—
			L	5.7	0.28	0.48	6.985	5.832	0.019	0.468	0.077	1.990
C	25	M	R	5.1	0.14	0.49	6.380	5.454	0.034	—	0.143	—
			L	5.0	0.12	0.49	6.401	5.296	0.061	—	0.256	—
D	25	M	R	6.0	0.34	0.44	7.872	6.093	0.048	—	0.218	—
			L	6.0	0.34	0.44	7.622	6.027	0.034	—	0.156	—
E	25	M	L	5.0	0.12	0.48	6.163	5.414	0.022	0.367	0.093	1.633
F	26	F	R	5.4	0.21	0.44	6.537	5.320	0.013	0.399	0.058	1.774
G	27	M	R	5.5	0.23	0.45	6.652	5.309	0.014	—	0.060	—
			L	5.7	0.28	0.45	7.306	5.524	0.039	—	0.175	—
H	29	F	R	5.7	0.28	0.41	7.185	5.906	0.032	—	0.155	—
			L	5.7	0.28	0.41	7.369	5.972	0.041	—	0.200	—
I	32	F	R	5.0	0.12	0.42	6.380	5.451	0.058	—	0.275	—
J	35	M	R	6.8	0.52	0.47	7.889	5.710	0.007	—	0.029	—
Mean				5.5	0.26	0.46	7.054	5.693	0.032	0.411	0.141	1.799
S.D.				0.5	0.11	0.03	0.563	0.289	0.017	0.051	0.079	0.180

BL<sub>T</sub>: Tooth BL thicknessBL<sub>P</sub>: Pulp BL thicknessBV<sub>F</sub>: Bloodvessel fraction in the pulp chamber

the periodontal tissue blood flow, including gingiva and periodontal ligament. Although previous researchers<sup>14</sup> reported that, because the tooth was surrounded by the periodontal tissue, which had abundant blood supply, the changes in the periodontal tissue blood flow might easily affect the TLP signal level, our experimental study where the silicone material was used to block the direct transmission of the light from the optical fiber placed against the palatal surface of the tooth, no statistically significant changes in both dc and ac/dc levels of the TLP signals with or without the silicone material were observed. Because the resin cap made for each volunteer had a close fit against the palatal surface, it might have helped to prevent light traveling toward the gingiva. In addition, because the newly developed TLP system employed the LED pulsed at 560 Hz, the background light, including 50 Hz noise, was removed to enhance the signal-to-noise ratio.<sup>16</sup> All these factors together probably resulted in improving the overall signal-to-noise ratio.

As for the light that had entered the tooth, which had traveled toward the gingiva and periodontal ligaments and that

had reflected back toward the pulp and finally toward the detector on the labial side, the Monte Carlo simulation has revealed that its effects were minimal. Of the  $2 \times 10^7$  photons injected from the palatal side into the tooth, the simulation showed only five photons or 0.000025% at 522 nm had reached the gingiva, reflected there, and finally reached the detector on the labial surface, while 497 photons or 0.0025% at 522 nm and 876 photons or 0.0044% at 810 nm, over 100 times the former, traveled straight to the detector through pulp without reaching the gingiva. The Monte Carlo simulation thus demonstrated minimal effects of the gingiva on the optical transmission measurements in the TLP.

On the basis of the experimental and theoretical studies as described above, we proceeded to develop a theoretical model to quantify pulp circulation. By simplifying the tooth structure, a TLM comprising dentin-pulp chamber-dentin layers was developed to analyze optical propagation in an extracted model tooth and to quantify effective hematocrit of the blood in the pulp chamber (Hct<sub>p</sub>). The Hct<sub>p</sub> was successfully quan-

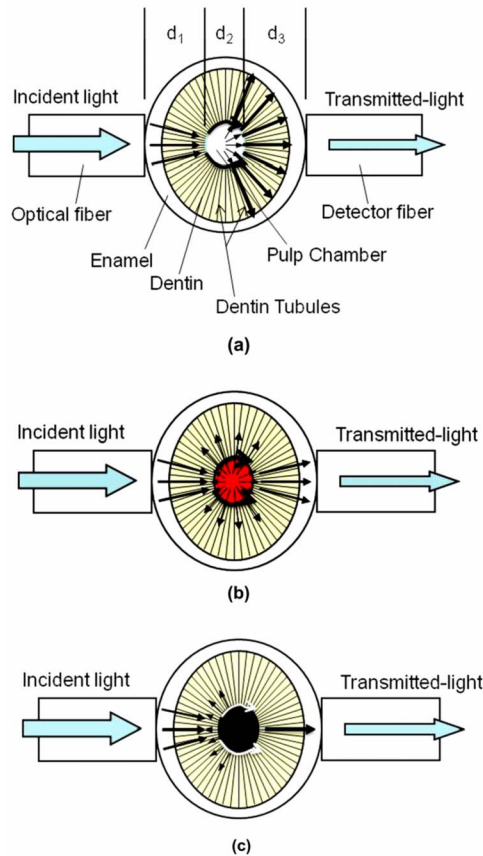


**Fig. 23** Summary of optical propagation patterns in the extracted model tooth, (a) with saline in the pulp chamber, (b) with a tenuous medium in the pulp chamber, and (c) with dense medium in the pulp chamber.

tified in the extracted model tooth using the 522 nm OD data in the TLM equation. The TLM equation was then applied to estimate  $Hct_p$  in the upper central incisors of 10 young human volunteers. The discussion here addresses (i) optical propagation in an extracted model tooth, (ii) TLM, (iii) quantification of  $Hct_p$  in the model tooth, (iv) estimation of  $Hct_p$  in human volunteers, and (v) assessment of dental pulp vitality from  $Hct_p$ .

### 5.1 Optical Propagation in an Extracted Model Tooth

The optical process in the extracted model tooth depended on the red blood cell concentration or  $Hct_p$ ,  $BL_p$ , and the light source wavelength. The wavelength-dependent absorption and scattering by hemoglobin and red blood cells in the pulp chamber and those of dentin layer determined the relation between the tooth's OD and  $Hct_p$ . Although the OD for 810 nm increased monotonously with its change of  $<1.0$  for  $Hct_p$  from 0.0 to 0.35 (Figs. 16 and 17), OD versus  $Hct_p$  curve at 522 nm comprised of two regions (Fig. 19), region I with  $Hct_p < 0.10$  and region II with  $Hct_p > 0.10$ . In the region I, OD increased by 1.0–3.0 as  $Hct_p$  increased from 0.0 to 0.10 with its rate and final level depending on the pulp chamber size, while  $>0.10$  it was similar to that of 810 nm.

In explaining the OD versus  $Hct_p$  curve of 522 nm, microscope pictures of Fig. 18 and summary graph of Fig. 23 were

helpful. When the pulp chamber had non-scattering fluid like saline [Figs. 18(a) and 23(a)], the light reaching the dentin-pulp chamber boundary propagated mainly in the forward direction with some photons scattered off along the boundary. The dentin tubules guided the light particles toward pulp chamber as well as from pulp chamber toward labial side of the tooth. When the pulp chamber had a tenuous medium with  $Hct_p < 0.10$ , photons entering the chamber were multiply scattered to propagate in all directions or absorbed by hemoglobin [Figs. 18(b) and 23(b)]. The OD level in the region I thus increased to reach a plateau as the  $Hct_p$  level increased to 0.10 because the photons penetrating the pulp chamber were reduced due to scattering and absorption. The OD level at plateau depends on the amount of photons routing around the pulp chamber to reach labial side. There was a large difference in OD level between the 522 and 810 nm wavelengths because of higher absorption at 522 nm,  $\sim 50$  times the 810 nm, and also larger scattering at 522 nm than 810 nm.

In region II with  $Hct_p > 0.10$ , as shown in Figs. 18(c) and 23(c), the light hitting the pulp chamber was completely blocked from advancing into the second dentin layer due to increased absorption as well as scattering in the pulp chamber. Only those photons that scattered off at the dentin-pulp chamber boundary and that routed around the pulp chamber probably reached the labial side. The light level at 522 nm wavelength beyond  $Hct_p$  of 0.10 is probably equal to the amount of photons routing around the pulp chamber. When the pulp chamber size was increased both in width and thickness, the amount of the light that was blocked by the pulp chamber increased simultaneously reducing the photons routing around the pulp chamber to consequently increase the OD level. When the pulp chamber size was narrowed to decrease the microvessel density, the OD level decreased with less attenuation of the light in the pulp chamber.

Comparison of the OD versus  $Hct_p$  characteristics of the 522 nm wavelength against those of 810 nm, where the pulp chamber was filled with whole blood or hemoglobin solution, suggested that in the region I extremely high absorption by hemoglobin determined the characteristics of the OD versus  $Hct_p$  curve at 522 nm wavelength although scattering had some effects, while at 810 nm wavelength the scattering was dominant in both regions, but its effect was much smaller in comparison to the absorption effect at 522 nm (Fig. 19).

### 5.2 TLM

In modeling the optical process in the extracted model tooth, particularly the effect of the blood volume change in the pulp chamber on the tooth's OD, the tooth structure was simplified to a TLM comprising dentin, pulp chamber, and dentin. The enamel layer had much lower scattering properties in comparison to the dentin tubules, and thus, it was excluded from the analysis.<sup>22,23</sup> The guided scattering by the dentin tubules as suggested by Kiele and Hibst and demonstrated by the Monte Carlo simulation in the preliminary study<sup>21</sup> was helpful in simplifying the model to a TLM. Although there were paths around the pulp chamber for the light to propagate, because of the tubule organization the light entering the dentin layer was mainly guided toward the pulp chamber. The microscope examination of optical process in the tooth revealed that some photons propagated along the dentin-pulp chamber boundary

to exit in the second dentin layer. The light propagating in the forward direction out of the pulp chamber was then guided along the dentin tubules spreading radially toward labial side.

The two-flux model proposed by Kubelka<sup>18,19</sup> was utilized to obtain an analytical equation relating the OD to tooth's dimensions, optical constants of each layer, and light-source wavelength. The optical constants of each layer were expressed by the bulk scattering and absorption constant,  $S$  and  $K$ , by assuming that each medium was optically homogeneous. For the dentin layer, the experimentally derived values were used,<sup>25</sup> while for the pulp chamber they were derived from the red blood cell properties and  $Hct_p$ . Because the scattering properties of the dentin layer depend on the dentin-tubule density, both scattering and absorption constants require adjustment from person to person.<sup>29,30</sup> In addition, optical properties of the model components including enamel, dentin, and pulp tissue vary with time due to growth, aging, pathological conditions, and discoloration due to surface characteristics, which, in turn, all affect the light transport through a tooth and absolute OD level.<sup>31</sup>

Concerning the boundary conditions for light transport in a complex medium, such as tooth, boundary conditions at the dentin-pulp chamber boundary need careful attention in improving the accuracy of the model, for the photons might be scattered off at the boundary depending on the ratio of the refractive indices between the dentin and pulp chamber. This effect was shown by the microscope examination where the light level at the dentin-pulp chamber boundary varied depending on the  $Hct_p$  level. If we assumed the index of refraction of the dentin to be 1.50 at 522 nm,<sup>32</sup> because that for the pulp chamber takes a value from 1.33 to 1.45 for the  $Hct_p$  level varying from 0.0 to 0.30, the ratio of the dentin to pulp chamber refractive indices changes from 1.13 to 1.03, the mismatch in index of refraction becoming lesser at higher  $Hct_p$  level. The ratio becomes closer to 1.0 at higher  $Hct_p$ , and hence, the absorption becomes a dominant factor for attenuating the light propagation at green wavelength, while for red and near-infrared wavelengths scattering is dominant to mask absorption. Hence there is a steady but small increase in the OD level. The OD versus  $Hct_p$  curves of 522 and 810 nm obtained in the extracted model tooth with its pulp chamber filled with whole blood or hemoglobin solution verified wavelength-dependent effects of scattering depending on the red blood cell concentration (Fig. 19).

Although the model yielded the qualitative description of the changes in the OD as a function of  $Hct_p$  and tooth dimensions, it required adjustment in the absolute level to quantify  $Hct_p$  of the dental pulp. In addition to improving the optical constants of the dentin and pulp chamber, the inclusion of the boundary condition, for example, such as  $p_1/p_2 = (n_1/n_2)^2$  at the boundary between layer 1 and 2 where  $p_1, p_2$  the photon densities and  $n_1, n_2$ , the index of refraction of the layer 1 and 2, respectively, as reported by Takatani et al.<sup>33</sup> for the two-layer model, could improve the quantitative accuracy of the model.

### 5.3 Quantification of $Hct_p$ in the Extracted Model Tooth

In connecting the experimental and theoretical studies, a method was developed to quantify  $Hct_p$  of the extracted

model tooth by utilizing the TLM equation. The difference in the absolute level between the experimental and theoretical OD was adjusted by calibrating the theoretical OD by the TLM against the experimental data of a selected reference tooth. After measuring the physical dimensions of the tooth, the tooth 4 with the  $BL_T$  and  $BL_p$  dimensions closest to the linear regression line of Fig. 12 was picked to obtain the gain constants required to normalize the theory to the experimental data. Although other teeth having dimensions not close to the regression line of Fig. 12 were tried, they did not yield results as good as tooth 4. For the  $Hct_p$  level of  $<0.10$ , where OD sensitivity to  $Hct_p$  change was much higher at 522 nm, it was possible to achieve a higher accuracy with mean error of  $-0.00115$ , while the mean error increased to  $+0.09157$  at 810 nm because of low sensitivity of OD with respect to  $Hct_p$ . As evident from the increasing SD values at higher  $Hct_p$  for both 522 and 810 nm wavelengths in Fig. 21, errors in  $Hct_p$  estimation based on the method described here increased because of the decreased sensitivity in OD versus  $Hct_p$  at higher  $Hct_p$  values.

### 5.4 Estimation of $Hct_p$ in Human Volunteers

In translating from the theory, to *ex vivo* study and finally to *in vivo* application, the TLM as calibrated by the *ex vivo* data was utilized to estimate  $Hct_p$  in 10 young volunteers. As summarized in Table 4, the mean  $Hct_p$  estimate in human volunteers based on the TLM was found to be 0.032 with a SD of 0.017. In our previous study,<sup>16</sup> we speculated the  $Hct_p$  *in vivo* from the following approximation:

$$Hct_p = Hct_{sys} \frac{Hct_{micro}}{Hct_{sys}} BV_F \quad (19)$$

where  $Hct_{sys}$  is the systemic large vessel hematocrit and  $Hct_{micro}$  is the microvessel hematocrit in the pulp chamber. Because the red blood cell concentration in the microvascular bed ranges from 46 to 53% of the larger vessels with the mean of  $\sim 50\%$ ,<sup>34</sup> we assumed  $Hct_{micro}/Hct_{sys}$  of 0.5. As for  $BV_F$ , Vongsavan and Mattheus<sup>35</sup> reported its value to be  $\sim 0.144$  from the cross-sectional analysis of the cat's canine tooth. When the  $BV_F$  of 0.144,  $Hct_{micro}/Hct_{sys}$  of 0.5 and  $Hct_{sys}$  value of each subject as determined from the blood sample were inserted in to the above equation,  $Hct_p$  estimate came to be 0.032, which is very close to the  $Hct_p$  estimate based on the TLM analysis. On the basis of the  $Hct_p$  estimate, the mean  $BV_F$  in 10 subjects came to be 0.141 with a SD of 0.079 (Table 4), showing excellent agreement with the value of 0.144 reported by Vongsavan and Matthews<sup>35</sup>

### 5.5 Assessment of Pulp Vitality by $Hct_p$

The mean  $Hct_p$  of the upper central incisor of human as estimated by the TLM agreed fairly well with the theoretical speculation assuming the systemic to microvascular hematocrit ratio of 0.50 as reported in the literature.<sup>34</sup> In addition, the effective fractional volume of the microvascular system  $BV_F$  was estimated to be 0.144 and again showed excellent agreement with the value measured from the cross section of the cat's canine tooth.<sup>35</sup> We thus here propose a new quantity " $Hct_p$  or  $BV_F$ " of the pulp chamber to assess microcirculatory changes related to dental pulp vitality.

On the basis of the TLP, the dental pulp vitality may be assessed using the light source wavelength in the green region most likely at the isosbestic wavelength of 522 nm. The measured signal can be processed in two ways, one in the pulse mode or the other absolute mode as reported in this study. The pulse mode can diagnose rapidly changing characteristics of the vascular system or compliance of the microvascular bed synchronized with the heartbeat, while the absolute mode can uncover accumulation or depletion of the blood in the dental pulp. The clinical diagnosis of circulatory status of dental pulp based on the absolute TLP should be established through accumulation of clinical data. In addition to the measurement of the absolute and time-varying blood volume at the isosbestic wavelength of 522 nm, the nonisosbestic wavelength of  $\sim 467$  nm, where the optical absorption is dependent on the oxygenation of the blood, can provide the average tissue oxygen level from which oxygen demand of the dental pulp may be assessed.<sup>16</sup> The determination of the blood volume shift in the pulp chamber by the isosbestic wavelength of 522 nm together with tissue oxygenation possibly determined from the nonisosbestic wavelength of 467 nm can provide the circulatory as well as metabolic dynamics reflecting vitality of the dental pulp.

## 6 Summary and Conclusion

Following the experimental and theoretical studies to verify that the periodontal circulation had little effect on TLP measurements, a TLM comprising dentin, pulp chamber, and dentin was developed to quantify pulp chamber hematocrit  $Hct_p$  of the human upper central incisors. The two-flux theory was used to derive a TLM equation in terms of tooth dimensions, pulp chamber  $Hct_p$ , and light-source wavelength, while its accuracy was tested in the extracted model tooth by varying the  $Hct_p$ . The optical transmission through the model tooth was measured at the isosbestic wavelengths of 522 and 810 nm. Although the TLM required one-point calibration using a reference tooth, the mean error defined as  $(Hct_p \text{ estimate} - \text{actual } Hct_p)$  in the model tooth was  $-0.00115$  with SD of 0.00733 at 522 nm, while at 810 nm they were  $+0.09157$  and 0.02493. The error at 810 nm was one order magnitude higher than that at 522 nm because of much lower sensitivity to  $Hct_p$  change at this wavelength. Finally, the TLM was applied to analyze the transmitted light intensity through the upper central incisors in young human volunteers. Although the optical properties of tooth might have varied from one person to the other and with time, one-point calibration in adjusting the TLM to that of a selected extracted tooth yielded the  $Hct_p$  estimate at 522 nm ranging from 0.007 to as high as 0.058 with the mean of 0.032. The analysis at 810 nm was not quite successful as 522 nm except in a few subjects because of much lower sensitivity of the optical density measurement at this wavelength. The effective fractional microvessel volume in the pulp chamber as derived from the  $Hct_p$  estimate, systemic blood hematocrit of each subject, and systemic to microvessel hematocrit ratio of 0.50 agreed well with the published result of 0.144. The noninvasive measurement of  $Hct_p$  or the fractional volume of microvessels occupied in the pulp chamber quantified by the method reported in this study can possibly provide clinically useful new information to assess vitality of dental pulp.

## Acknowledgments

The authors acknowledge cooperation and valuable suggestions provided by Dr. Z. Miwa, Dr. A. Kirimoto, and Dr. K. Ohuchi of Tokyo Medical and Dental University, Tokyo, Dr. T. Yasuda of Yamaguchi University, Yamaguchi, and H. Yoshihara and M. Murata of Opt-Techno Inc., Kanagawa, Japan, for their kind support of the project.

## References

1. H. J. Fulling and J. O. Andreasen, "Influence of maturation status and tooth type of permanent teeth upon electrometric and thermal pulp testing," *Scand. J. Dent. Res.* **84**, 286–290 (1976).
2. H. Klein, "Pulp responses to an electric pulp stimulator in the developing permanent anterior dentition," *ASDC J. Dent. Child.* **45**, 199–202 (1978).
3. D. D. Upthegrove, J. G. Bishop, and H. L. Dorman, "A method for detecting of blood flow in the dental pulp," *J. Dent. Res.* **45**, 1115–1119 (1966).
4. G. Beer, H. Negari, and S. Samueloff, "Feline dental pulp photoplethysmography during stimulation of vasomotor nerve supply," *Arch. Oral Biol.* **19**, 81–86 (1974).
5. B. Gazelius, L. Olgart, B. Edwall, and L. Edwall, "Noninvasive recording of blood flow in human dental pulp," *Endod. Dent. Traumatol.* **2**, 219–221 (1986).
6. B. Gazelius, L. Olgart, and B. Edwall, "Restored vitality in luxated teeth assessed by Laser Doppler flowmeter," *Endod. Dent. Traumatol.* **4**, 265–268 (1988).
7. J. M. Schmitt, R. L. Webber, and E. C. Walker, "Optical determination of dental pulp vitality," *IEEE Trans. Biomed. Eng.* **38**, 346–352 (1991).
8. W. C. Nobletto, L. R. Wilcox, F. Scamman, W. T. Johnson, and A. Diaz-Arnold, "Detection of pulpal circulation *in vitro* by pulse oximetry," *J. Endod.* **22**(1), 1–5 (1996).
9. A. K. Munshi, A. M. Hegde, and S. Radhakrishnan, "Pulse Oximetry: a diagnostic instrument in pulpal vitality testing," *J. Clin. Pediatr. Dent.* **26**(2), 141–145 (2002).
10. I. Shohar, Y. Mahler, and S. Samueloff, "Dental pulp photoplethysmography in human being," *J. Oral Surg.* **36**, 915–921 (1973).
11. M. Ikawa, H. Horiuchi, and K. Ikawa, "Optical characteristics of human extracted teeth and the possible application of photoplethysmography to the human pulp," *Arch. Oral Biol.* **39**, 821–827 (1994).
12. A. Diaz-Arnold, L. R. Wilcox, and M. Arnold, "Optical detection of pulpal blood," *J. Endod.* **20**(4), 164–168 (1994).
13. A. Diaz-Arnold, M. Arnold, and L. R. Wilcox, "Optical detection of hemoglobin in pulpal blood," *J. Endod.* **22**(1), 19–22 (1996).
14. M. E. Fein, A. H. Gluskin, W. W. Y. Goon, B. B. Chew, W. A. Crone, and H. W. Jones, "Evaluation of optical methods of detecting dental pulp vitality," *J. Biomed. Opt.* **2**, 58–73 (1997).
15. Z. Miwa, M. Ikawa, H. Iijima, M. Saito, and Y. Takagi, "Pulpal blood flow in vital and nonvital young permanent teeth measured by transmitted light photoplethysmography: A pilot study," *Pediatr. Dent.* **24**(6), 594–598 (2002).
16. S. Kakino, Z. Miwa, A. Kirimoto, K. Ohuchi, S. Takatani, and Y. Takagi, "A new multi-wavelength optical plethysmograph for quantitative determination of pulpal hemoglobin content and oxygen level using green and near-infrared LEDs," *Proc. SPIE* **6425**, 642508 (2007).
17. L. Wang, L. S. Jacques, and L. Zheng, "MCML—Monte Carlo modeling of light transport in multi-layered tissues," *Comput. Methods Programs Biomed.* **47**, 131–146 (1995).
18. P. Kubelka, "New contribution to the optics of intensely light-scattering materials. Part I," *J. Opt. Soc. Am.* **38**, 457–448 (1948).
19. P. Kubelka, "New contributions to the optics of intensely light-scattering materials. Part II: Nonhomogeneous layers," *J. Opt. Soc. Am.* **44**(4), 330–335 (1954).
20. A. Kienle, R. Michels, and R. Hibst, "Magnification—A new look at a long-known optical property of dentin," *J. Dent. Res.* **85**(10), 955–959 (2006).
21. A. Kiele and R. Hibst, "Light guiding in biological tissue due to scattering," *Phys. Rev. Lett.* **97**, 018104 (2006).
22. D. Spitzer and J. J. T. Bosch, "The absorption and scattering of light in bovine and human dental enamel," *Calcif. Tissue Res.* **17**, 129–137 (1975).

23. J. R. Zijp and J. J. T. Bosch, "Theoretical model for the scattering of light by dentin and comparison with measurements," *Appl. Opt.* **32**(4), 411–415 (1993).
24. B. L. Horecker, "The absorption spectra of hemoglobin and its derivatives in the visible and near infrared regions," *J. Biol. Chem.* **48**, 173–183 (1943).
25. D. Fried, R. E. Glens, J. D. B. Featherstone, and W. Seka, "Nature of light scattering in dental enamel and dentin at visible and near-infrared wavelengths," *Appl. Opt.* **34**(7), 1278–1285 (1995).
26. V. Twersky, "Absorption and multiple scattering by biological suspensions," *J. Opt. Soc. Am.* **60**(8), 1084–1093 (1970).
27. J. Bartminn, "Design and evaluation of a hybrid optical reflectance oxygen saturation and haemoglobin content sensor for mechanical total artificial heart control," Master's thesis, Aachen Technical University, Aachen, Germany (1998).
28. S. Takatani, "On the theory and development of a noninvasive tissue reflectance oximeter," PhD dissertation, Department of Biomedical Engineering, Case Western Reserve University, Cleveland, OH (1979).
29. J. J. ten Bosch and J. R. Zijp, "Optical properties of dentin" in *Dentin and Dentin Reactions in the Oral Cavity*, A. Thylstrup, S. A. Leach, and V. Qvist, Eds., pp. 59–65, IRL Press, Oxford, (1987).
30. J. Vaarkamp, J. J. ten Bosch, and E. H. Verdonshot, "Propagation of light through human dental enamel and dentin," *Caries Res.* **29**(8), 8–13 (1995).
31. J. J. ten Bosch and J. C. Coops, "Tooth color and reflectance a related to light scattering and enamelhardness," *J. Dent. Res.* **74**(1), 374–380 (1995).
32. X. J. Wang, T. E. Milner, J. F. deBoer, Y. Zhang, D. H. Pashley, and J. S. Nelson, "Characterization of dentin and enamel by use of optical coherence tomography," *Appl. Opt.* **38**(10), 2092–2096 (1999).
33. S. Takatani and M. D. Graham, "Theoretical analysis of diffuse reflectance from a two-layer tissue model," *IEEE Trans. Biomed. Eng.* **216**(12), 656–664 (1979).
34. B. W. Zweifach and H. H. Lipowsky, "Pressure-flow relations in blood and lymph microcirculation," in *Handbook of Physiology: Cardiovascular System*, E. M. Renkin, C. C. Michel, and S. R. Geiger, Eds., Vol. 4, pp. 251–307, American Physiological Society, Bethesda, (1984).
35. N. Vongsavan and B. Matthews, "The vascularity of dental pulp in cats," *J. Dent. Res.* **71**(12), 1913–1915 (1992).